Epidermis-Type Lipoxygenase 3 Regulates Adipocyte Differentiation and Peroxisome Proliferator-Activated Receptor γ Activity[▽][†]

Philip Hallenborg,[1,9][‡] Claus Jørgensen,[1][‡] Rasmus K. Petersen,[1,2,9] Søren Feddersen,[1] Pedro Araujo,[3]
Patrick Markt,[4] Thierry Langer,[4] Gerhard Furstenberger,[5] Peter Krieg,[5] Arjen Koppen,[6,7]
Eric Kalkhoven,[6,7,8] Lise Madsen,[3,9] and Karsten Kristiansen[9]*

*Department of Biochemistry and Molecular Biology, University of Southern Denmark, Odense, Denmark[1]; BioLigands,
International Science Park Odense, Odense, Denmark[2]; National Institute of Nutrition and Seafood Research, Bergen,
Norway[3]; Department of Pharmaceutical Chemistry, University of Innsbruck, Innsbruck, Austria[4]; Genome Modifications and
Carcinogenesis, German Cancer Research Center Heidelberg, Heidelberg, Germany[5]; Department of Metabolic and
Endocrine Diseases, University Medical Center Utrecht, Utrecht, Netherlands[6]; Netherlands Metabolomics Center,
Leiden, Netherlands[7]; Department of Pediatric Immunology, University Medical Center Utrecht, Utrecht,
Netherlands[8]; and Department of Biology, University of Copenhagen, Copenhagen, Denmark[9]*

The nuclear receptor peroxisome proliferator-activated receptor γ (PPARγ) is essential for adipogenesis. Although several fatty acids and their derivatives are known to bind and activate PPARγ, the nature of the endogenous ligand(s) promoting the early stages of adipocyte differentiation has remained enigmatic. Previously, we showed that lipoxygenase (LOX) activity is involved in activation of PPARγ during the early stages of adipocyte differentiation. Of the seven known murine LOXs, only the unconventional LOX epidermis-type lipoxygenase 3 (eLOX3) is expressed in 3T3-L1 preadipocytes. Here, we show that forced expression of eLOX3 or addition of eLOX3 products stimulated adipogenesis under conditions that normally require an exogenous PPARγ ligand for differentiation. Hepoxilins, a group of oxidized arachidonic acid derivatives produced by eLOX3, bound to and activated PPARγ. Production of hepoxilins was increased transiently during the initial stages of adipogenesis. Furthermore, small interfering RNA-mediated or retroviral short hairpin RNA-mediated knockdown of eLOX3 expression abolished differentiation of 3T3-L1 preadipocytes. Finally, we demonstrate that xanthine oxidoreductase (XOR) and eLOX3 synergistically enhanced PPARγ-mediated transactivation. Collectively, our results indicate that hepoxilins produced by the concerted action of XOR and eLOX3 may function as PPARγ activators capable of promoting the early PPARγ-dependent steps in the conversion of preadipocytes into adipocytes.

Differentiation of preadipocytes into mature fat-laden insulin-responsive adipocytes is a complex process involving the sequential activation of several transcription factors (46). The activity of the nuclear hormone receptor peroxisome proliferator-activated receptor γ (PPARγ) is essential for adipogenic conversion (16, 44), and PPARγ antagonists block adipocyte differentiation (10, 41, 54). Production of endogenous PPARγ activator(s) peaks within the first 2 days after cells are induced to undergo adipocyte differentiation (35, 54). Furthermore, elevation of cyclic AMP (cAMP) levels is important for the regulated production of an endogenous PPARγ activator (54), a process suggested to be dependent on CCAAT/enhancer-binding protein β (C/EBPβ) activity (20). The positive effect of C/EBPβ on PPARγ ligand production was recently demonstrated to involve induction of xanthine oxidoreductase (XOR) expression (13). XOR was originally linked to purine catabolism but has also been associated with the generation of reactive oxygen species (ROS). Interestingly, blocking the site in

XOR responsible for ROS generation abolishes its ligand-producing ability (13).

In addition to C/EBPβ, adipocyte differentiation can be induced by the sterol regulatory element binding protein-1c (SREBP-1c)/adipocyte determination and differentiation-dependent factor 1 (ADD1) by a mechanism that at least in part involves induced biosynthesis of an endogenous PPARγ activator. The nature of this compound still remains unknown (26).

PPARγ is activated by a structurally diverse array of natural and synthetic compounds, such as the insulin-sensitizing thiazolidinediones (TZDs) (30, 33). Naturally occurring compounds that activate PPARγ and stimulate adipose conversion comprise polyunsaturated fatty acids (PUFAs) and fatty acid-derived compounds such as 15-deoxy-$\Delta^{12,14}$-prostaglandin J_2 (15-dPGJ$_2$), hydroxyeicosatetraenoic acids (8-HETE and 15-HETE), and hydroxyoctadecadienoic acids (9-HODE and 13-HODE) (17, 23, 28–30, 38, 53, 57, 61). Although capable of activating PPARγ, none of these fatty acids has been demonstrated to accumulate during the early stages of adipocyte differentiation.

Lipoxygenases (LOXs) catalyze the dioxygenation of cognate lipid substrates in a stereo- and regioselective manner, using a non-heme iron as a cofactor. Several PUFAs have been shown to act as potential LOX substrates (60). LOXs constitute a large family of enzymes, and the latest addition

is the epidermal-type lipoxygenase 3 (eLOX3) (27). In contrast to previously characterized LOXs, eLOX3 functions as a hydroperoxide isomerase, converting the LOX products hydroperoxyeicosatetraenoic acids (HPETEs) to hepoxilin-like products. Curiously, whereas human eLOX3 prefers 12-HPETEs as substrates, mouse eLOX3 favors 5- and 8-HPETEs although both human and mouse eLOX3 have the capability to isomerize a broad spectrum of HPETEs (63, 65). The fact that inactivating mutations in either the 12R-LOX gene or the eLOX3 gene are found in patients suffering from the skin disease nonbullous congenital ichthyosiform erythroderma underscores the requirement for a functioning LOX upstream of eLOX3 in skin (25, 62).

Previously, we demonstrated that LOX activity is required for differentiation of 3T3-L1 preadipocytes by showing that adipocyte differentiation is blocked by the LOX inhibitor baicalein (35). Addition of the PPARγ agonist rosiglitazone to baicalein-treated 3T3-L1 preadipocytes restored adipocyte differentiation, suggesting that LOX activity precedes PPARγ activation. Surprisingly, we found that although several LOXs are expressed in adipose tissue, only the unconventional eLOX3 is expressed in 3T3-L1 preadipocytes. Here, we show that eLOX3 activity is required for differentiation of 3T3-L1 preadipocytes. We present evidence that hepoxilins accumulate during the initial stages of the conversion of 3T3-L1 preadipocytes into adipocytes and that hepoxilins can activate PPARγ and promote adipocyte differentiation. Finally, we demonstrate that eLOX3 and XOR, which can produce HPETE substrates for eLOX3, synergistically enhance PPARγ-mediated transactivation, suggesting a mechanism by which enzymatic production of endogenous PPARγ activators can promote the initiation of adipocyte differentiation.

MATERIALS AND METHODS

Plasmids. Mouse eLOX3 was cloned into pcDNA3.1 (Invitrogen) and pBABE (generously provided by Ormond MacDougald) by PCR. Deletion of amino acids (aa) N155 to P195 and generation of myc-tagged eLOX3 were performed by PCR. All clones were verified by sequencing. pBABE-ADD1R was a generous gift from Bruce M. Spiegelman. UASGal-TK-Luc (where UAS is upstream activator sequence, TK is thymidine kinase, and Luc is luciferase) was kindly provided by Ronald M. Evans. The cytomegalovirus (CMV)-β-galactosidase was from Clontech. Gal4-PPARα, -PPARδ, and -PPARγ ligand binding domains (LBD) were kindly donated by Jan Fleckner (Novo Nordisk A/S). Gal4-retinoid X receptor α (RXRα) LBD contains the rat RXRα LBD (aa 202 to 467) cloned in frame to the Gal4 DNA-binding domain (DBD) in pM (Clontech). pDR1 Luc, MSCV-PPARγ (where MSCV is murine stem cell virus), and MSCV-PPARγ Q286P were generous gifts from Bruce M. Spiegelman. pcDNA3.1mychisA XOR was a generous gift from Toren Finkel. Enhanced green fluorescent protein (EGFP)-PPARγ was constructed by cloning full-length PPARγ in frame to EGFP in CMV-EGFP (Stratagene). The PPARγ-DE domains were inserted into pGEX-5x-1 (GE Healthcare) placing a glutathione S-transferase (GST) tag in the N terminus of the PPARγ fragment. pCMX-T7-TRAP220 was generously provided by Eckhardt Treuter. pSUPER-RETRO was kindly supplied by Reuven Agami. Target sequences for eLOX3 were identified using a small interfering RNA (siRNA) target identifier from Ambion (Austin, TX). Oligonucleotides were annealed and cloned into pSUPER-RETRO. The following target sequences were used: GTATCTCACCGCAATCATC, AAGACCTTCACTTC AGAGTAC, and AATCATCTTTAATTGCTCCGC.

Cell culture, differentiation, transduction, siRNA transfection, and oil red O staining. Wild-type mouse embryonic fibroblasts (MEFs) and MEFs lacking a functional retinoblastoma tumor suppressor gene ($Rb^{-/-}$) were generous gifts from Jiri Bartek and Jiri Lukas. MEFs and 3T3-L1 preadipocytes were grown, differentiated, and transduced as described previously (21). For the hepoxilin differentiation experiments, vehicle or hepoxilins at a 4 or 10 μM final concen-

tration were added to differentiation medium at days 0, 1, 2, and 3. N-Acetylcysteine (NAC) was dissolved in water and vehicle, or NAC (5 mM) was added to the differentiation medium for the periods indicated in the Fig. 7 legend. eLOX3 SMART pool RNA interference (RNAi) (Dharmacon) was transfected into 3T3-L1 cells at confluence, using DeliverX plus (Panomics) according to the manufacturer's instructions. For oil red O staining, plates were washed in phosphate-buffered saline (PBS), and cells were fixed in 3.7% paraformaldehyde for 1 h and stained as described previously (21).

Immunofluorescence analysis. EGFP-PPARγ and myc-eLOX3 were transfected into 50% confluent 3T3-L1 cells using Metafectene (Biontex). After 24 h, cells were washed twice in PBS, pH 7.2, and fixed with 90% methanol at −20°C. Following fixation, cells were washed in PBS, pH 7.2, and blocked for 1 h at room temperature in 3% horse serum (HS)-PBS. Incubation with monoclonal anti-myc antibody (Roche 9E10) was performed at a 1:50 dilution in 3% HS-PBS for 1 h at room temperature. Cells were subsequently washed in PBS, pH 7.2, and incubated with a Cy3-conjugated anti-mouse antibody (Jackson ImmunoLabs) at 1:250 for 1 h at room temperature. Finally, cells were washed and mounted using fluorescent mounting medium (Dako). Visualization was performed on a Zeiss Axiovert 200 M laser scanning confocal microscope with a pinhole of 1, and scanning was performed within selected ranges of 495 to 548 nm for EGFP and from 580 nm for Cy3. Image processing was performed with Zeiss software.

Real-time PCR and protein analysis. Total RNA was purified as described previously (21). Prior to reverse transcription, RNA was treated with RQ1 DNase (Promega), and reverse transcription was performed essentially as described previously (35). Expression levels of genes of interest were normalized to expression of the TATA box-binding protein (TBP). Primer sequences are available on request.

For protein analysis, whole-cell extracts, electrophoresis, blotting, visualization, and stripping of membranes were performed as described previously (21). Primary antibodies were rabbit anti-eLOX3 (35), mouse anti-PPARγ (Santa Cruz sc-7273), rabbit anti-GLUT1 (Abcam ab652), rabbit anti-GLUT4 (Abcam ab654), rabbit anti-TFIIB (Santa Cruz sc-274), and rabbit anti-aP2 (kindly provided by David A. Bernlohr). Secondary antibodies were horseradish peroxidase-conjugated anti-rabbit and anti-mouse antibodies from Dako.

LOX activity assay and detection of HETEs by enzyme-linked immunosorbent assay (ELISA). Detection of LOX activity was performed essentially as described previously (9, 52) with increasing amounts of baicalein added to the enzymatic reaction as indicated in Fig. 2D.

ELISAs for the specific detection of 12(S)-HETE and 15(S)-HETE were from R&D Systems and were used according to the manufacturer's instructions. Briefly, organic extracts of medium from 3T3-L1 preadipocytes were loaded on C_{18} columns. Fractions from ethyl acetate elutions were evaporated to dryness, resuspended in ethanol, and assayed.

Transfections. Sixty percent confluent $Rb^{-/-}$ MEFs were transfected using Metafectene (Biontex) according to the manufacturer's instructions. Six hours after transfection, medium was changed to AmnioMax basal medium supplemented with antibiotics and hepoxilin A3 (HXA3), hepoxilin B3 (HXB3) (Biomol), L165041 (kindly provided by Merck), rosiglitazone (kindly supplied by Novo Nordisk A/S), or LG1069 (kindly supplied by Novo Nordisk A/S). All compounds were dissolved in dimethyl sulfoxide (DMSO) or ethanol. Where no compounds were added, an equal volume of vehicle was added. Cells were harvested after 12 h, and luciferase and β-galactosidase activities were measured according to standard protocols.

Insulin-stimulated glucose uptake. Glucose uptake was measured in 3T3-L1 adipocytes. On day 6 of differentiation, the cells were treated with vehicle, rosiglitazone, or hepoxilins. Forty-eight hours later the cells were incubated with serum-free Dulbecco's modified Eagle's medium (DMEM) supplemented with antibiotics at 37°C for 1 to 2 h. Afterwards, the cells were washed once with Krebs-Ringer-HEPES (KRP) buffer and incubated with KRP buffer for 30 min at 37°C. Insulin was added to a final concentration of 0, 10, or 100 nM, and cells were incubated at 37°C for 15 min. Glucose uptake was initiated by the addition of 100 μl of KRP buffer supplemented with 10 mM glucose (5 mCi/liter 2-deoxy-D-[^{14}C]glucose), and cells were incubated for 10 min at 37°C. Glucose uptake was terminated by three washes with ice-cold PBS. The cells were lysed with 1% Triton X-100, scintillation fluid was added, and radioactivity was determined.

Liquid chromatography mass spectrometry (LC/MS). Sample preparation and instrument setup were performed as described previously (1). Screening was carried out by fragmenting the ion [M-H]$^-$ signal m/z 335.1 (M is hepoxilin A3 or B3) and monitoring the transitions at [M-H₂O-H]$^-$ signal m/z 317, [M-2H₂O-H]$^-$ signal m/z 299, [M-COO-H]$^-$ signal m/z 291, [M-H₂O-COO-H]$^-$ signal m/z
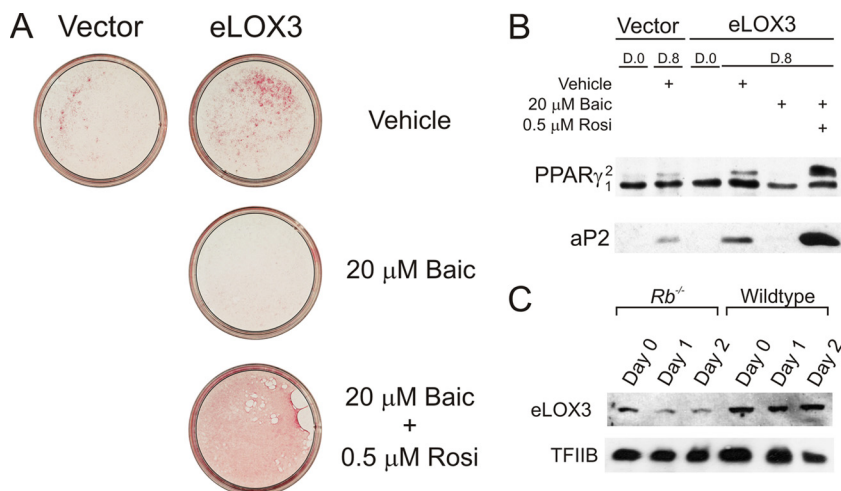
FIG. 1. Forced expression of eLOX3 increases differentiation of $Rb^{-/-}$ MEFs. Cells were transduced with either an empty or eLOX3-expressing vector and selected using puromycin. Cells were induced to differentiate according to the MDI protocol with the inclusion of either vehicle, 20 μM baicalein, or 20 μM baicalein and 0.5 μM rosiglitazone from time of induction. Eight days after induction, cells were scored for differentiation. (A) Cells stained for lipid accumulation using oil red O. (B) Expression of adipocyte marker genes, PPARγ2 and aP2, was analyzed by Western blotting. (C) Protein levels of eLOX3 in wild-type and $Rb^{-/-}$ MEFs at the onset of differentiation as analyzed by Western blotting. TFIIB was included as a loading control. One representative experiment out of three independent experiments performed in duplicate is shown.

273, and $[\text{M-2H}_2\text{O-COO-H}]^-$ signal m/z 255. The intensities of the signals were recorded in ion counts per second (icps).

Ligand binding assay. A LanthaScreen time-resolved fluorescence resonance energy transfer (TR-FRET) PPARγ competitive binding assay (Invitrogen) was used according to the manufacturer's instructions with increasing concentrations of hepoxilin A3, hepoxilin B3, or rosiglitazone, as indicated in Fig. 4B.

GST pulldown. GST-PPARγ DE was expressed in *Escherichia coli* by induction with 0.1 mM isopropyl-β-ᴅ-thiogalactosidase at 30°C. Cells were disrupted by sonication, and the cell lysate was subsequently incubated with glutathione-Sepharose (GE Healthcare). The TRAP220 fragment was produced by *in vitro* translation (TnT; Promega) in the presence of [^{35}S]methionine (Amersham). Beads and *in vitro* translated proteins were incubated in pulldown buffer (20 mM Tris-HCl, pH 8.0, 100 mM NaCl, 10 mM EDTA, 0.5% NP-40, 1% skim milk, and protease inhibitors [Complete; Roche]) for 15 min at 4°C in the presence of vehicle, rosiglitazone, HXA3, or HXB3. Beads were washed once with pulldown buffer containing skim milk and twice with pulldown buffer without skim milk. All buffers contained vehicle or ligands. Beads were then boiled in SDS lysis buffer and resolved using SDS-PAGE. [^{35}S]methionine-labeled proteins were visualized by autoradiography.

Docking of hepoxilins. To model docking of hepoxilin A3 and B3 to the PPARγ ligand-binding pocket, the Gold Suite software package was applied (CCDC Gold Suite, Cambridge, United Kingdom). The two hepoxilins were prepared using Corina, version 3.00 (Molecular Networks, Erlangen, Germany), for generating three-dimensional structures, Omega, version 2.2.1 (Openeye Scientific Software Inc., Santa Fe, NM), for energy minimization, and Open Babel, version 2.1.0 (http://openbabel.sourceforge.net/), for calculating protonation states at physiological pH. Sybyl, version 8.0 (Tripos, St. Louis, MO), was applied for protein preparation. The Brookhaven Protein Data Bank (PDB) was searched for crystallographic data of agonist-PPARγ complexes (7). Among the agonist-PPARγ complexes that included two fatty acids bound simultaneously in the ligand-binding domain, the PDB entry 2vsr had the highest crystal structure resolution, so its PPARγ ligand-binding pocket was chosen to set up a docking protocol. The resulting docking poses were visualized with LigandScout, version 2.0 (56). The best docking poses were determined with respect to their GOLD-Scores and plausibility. For example, a docking pose that represented known agonist-PPARγ interactions and was ranked second in terms of GOLDScore was preferred over the highest-ranked docking pose that formed mostly implausible ligand-protein interactions.

Data presentation. All data shown are representatives of at least two independent experiments performed at least in duplicate. All error bars represent standard deviations.

RESULTS

eLOX3 promotes adipocyte differentiation of $Rb^{-/-}$ mouse embryonic fibroblasts (MEFs). We previously showed that LOX inhibitors prevented adipogenesis if added during the early stages of 3T3-L1 adipocyte differentiation and that this inhibition was circumvented by the addition of a PPARγ agonist (35). These findings suggested a LOX-dependent activation of PPARγ during the initiation of adipocyte differentiation, implicating the unconventional LOX, eLOX3, in the process since this is the only LOX detectable in differentiating 3T3-L1 preadipocytes (35).

To investigate the possible role of eLOX3 in activation of PPARγ, we used $Rb^{-/-}$ MEFs as a model system. Whereas more than 90% of 3T3-L1 preadipocytes differentiate when induced by the standard methylisobutylxanthine, dexamethasone, and insulin (MDI) protocol, $Rb^{-/-}$ MEFs require a PPARγ agonist in the differentiation cocktail in order to undergo adipose conversion (21). $Rb^{-/-}$ MEFs are furthermore a particularly sensitive system for detecting PPARγ ligands as the retinoblastoma protein (pRB) is a PPARγ corepressor (15). Therefore, we initially used $Rb^{-/-}$ MEFs as a model for identification of enzymes and pathways involved in activation of PPARγ and, hence, possibly PPARγ ligand production.

$Rb^{-/-}$ MEFs were transduced with a retroviral vector encoding eLOX3 or empty vector, selected, and differentiated according to the MDI protocol. Vector control cells barely differentiated, but cells expressing eLOX3 underwent adipocyte differentiation as seen by increased oil red O staining (Fig. 1A) and expression of the adipocyte marker genes aP2 and PPARγ2 (Fig. 1B). As observed for 3T3-L1 preadipocytes (35), addition of the LOX inhibitor baicalein from the time of induction and throughout the differentiation period prevented differentiation of $Rb^{-/-}$ MEFs with forced expression of
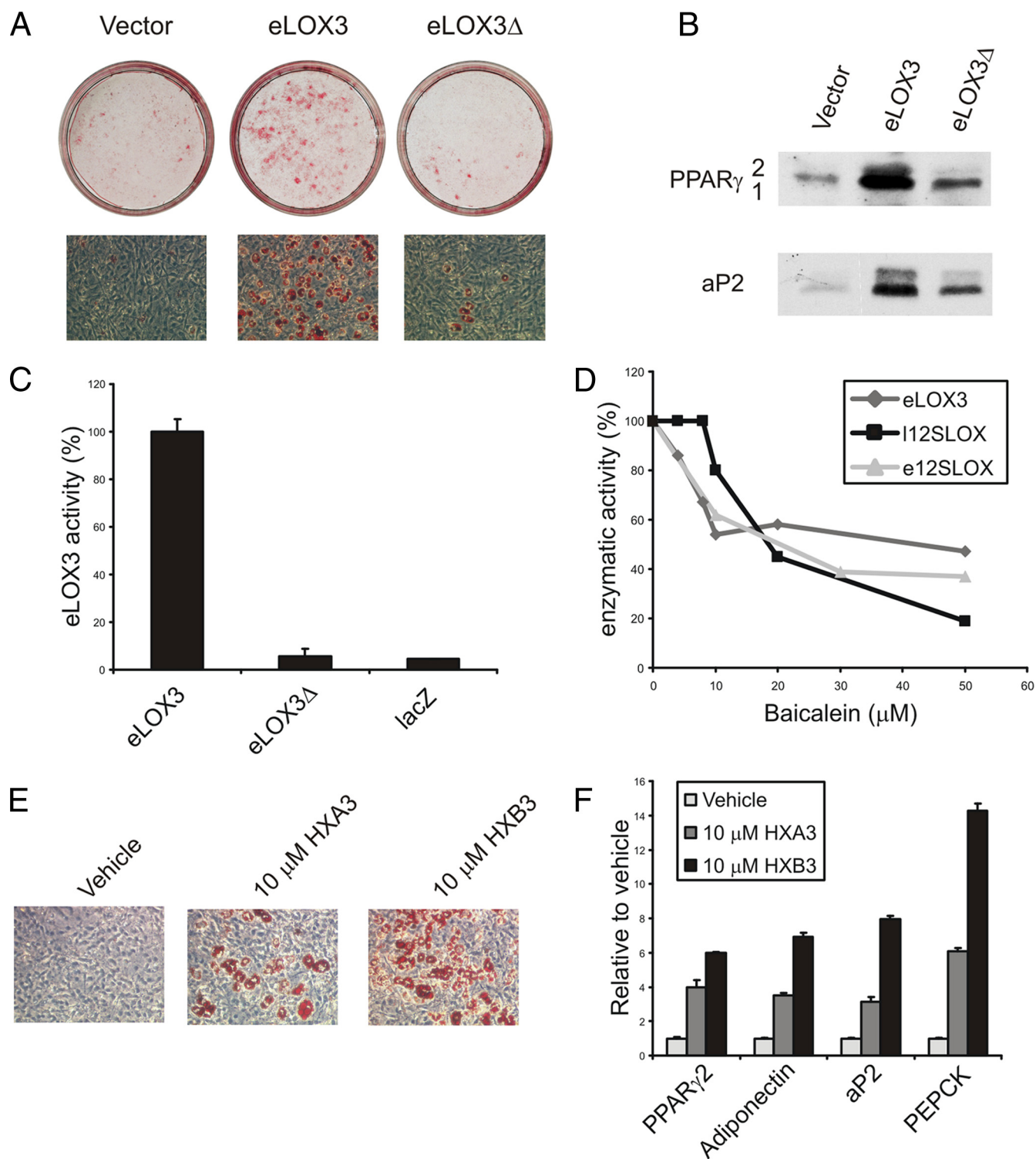
FIG. 2. The enzymatic activity of eLOX3 is required for its adipogenic effect. $Rb^{-/-}$ MEFs were transduced with vectors expressing eLOX3, the eLOX3Δ inactive mutant, or vector control and selected using puromycin. Eight days after induction with MDI, cells were scored for adipogenic conversion. (A) Cells were stained for lipid accumulation using oil red O. (B) Expression of adipocyte marker genes, PPARγ and aP2, was analyzed by Western blotting. Data are representative of three independent experiments performed in duplicate. (C) Enzymatic properties of the eLOX3Δ mutant. Cells were transiently transfected with wild-type eLOX3, eLOX3Δ, or LacZ control expression vectors, lysed in LOX assay buffer, and incubated with 100 μM 15(S)-HPETE for 15 min at 37°C. Products were extracted and run on a high-performance liquid chromatograph, and eluates were monitored at 205 nM. Depicted is conversion of 15(S)-HPETE into 13(R)-hydroxy-14(S),15(S)-HepEtrE with the activity of wild-type eLOX3 set to 100%. Data are representative of two independent experiments. (D) Baicalein inhibits enzymatic activity of known LOXs. Expression vectors harboring cDNAs encoding different LOXs were transiently transfected into 293 cells. Cells were lysed in LOX assay buffer and incubated with appropriate substrate and increasing amounts of baicalein. Enzymatic activation is depicted as percent activity with activation in the absence

eLOX3 (Fig. 1A and B). If baicalein abolished adipocyte differentiation by inhibiting eLOX3 activity and eLOX3 activity preceded PPARγ activation, we predicted that inclusion of the PPARγ-specific agonist rosiglitazone would overcome the inhibitory effect of baicalein. Indeed, addition of rosiglitazone rescued adipocyte differentiation of baicalein-treated $Rb^{-/-}$ MEFs overexpressing eLOX3 (Fig. 1A and B). These results show that eLOX3 induced differentiation in a model system that would otherwise require addition of an exogenous PPARγ activator. To investigate if eLOX3 expression was perturbed in $Rb^{-/-}$ MEFs and to test if reintroduction of eLOX3 at least in part augmented adipogenesis by restoring eLOX3 expression levels, we examined eLOX3 protein levels by immunoblotting. Intriguingly, eLOX3 levels were decreased in $Rb^{-/-}$ MEFs compared to levels in wild-type MEFs (Fig. 1C), suggesting that low expression of eLOX3 in $Rb^{-/-}$ MEFs contributed to their impaired ability to undergo adipocyte differentiation.

ADD1 has been implicated in the production of PPARγ ligands (26), but the mechanism by which ADD1 leads to increased PPARγ ligand production has not been elucidated. Using transient transfections, we observed that ADD1 induced the expression of a luciferase reporter gene controlled by a 2.5-kb fragment of the eLOX3 promoter (data not shown), indicating that augmentation of eLOX3 expression might underlie ligand production in response to forced expression of ADD1. To further examine this possibility, we transduced $Rb^{-/-}$ MEFs with a retroviral vector expressing the E-box-selective ADD1 mutant (ADD1R), previously shown to be as efficient as wild-type ADD1 in inducing PPARγ ligand production (26). Forced expression of ADD1R, indeed, caused adipogenesis in $Rb^{-/-}$ MEFs. This effect was abolished by the addition of baicalein, but not indomethacin, a cyclooxygenase inhibitor. Addition of rosiglitazone to the baicalein-treated cells rescued differentiation (see Fig. S1A to D in the supplemental material). Collectively, these results indicated that forced expression of ADD1R may promote PPARγ ligand production and adipogenesis in a LOX-dependent manner, underscoring the ability of LOXs to promote adipogenesis *in vitro*. However, two points strongly argue against the idea that ligand production induced by forced expression of ADD1R reflects the mechanism for ligand generation and activation of PPARγ during normal adipocyte differentiation. eLOX3 mRNA decreases upon induction of adipocyte differentiation, which is opposite to the increase in ADD1 expression. Whereas eLOX3 mRNA drops at the onset of adipogenesis, the eLOX3 protein level remains stable, suggesting that eLOX3 activity is regulated by other means than increased mRNA expression. Besides augmenting eLOX3 mRNA levels, forced expression of ADD1R also induced expression of platelet-type 12(S)-LOX (p12SLOX) (see Fig. S1E in the supplemental material), an enzyme with the ability to produce substrates for eLOX3. Expression of p12SLOX is, however,

undetectable in 3T3-L1 cells (35), which disagrees with the assumption that this enzyme is the one responsible for generating substrates for eLOX3 during adipogenesis.

eLOX3 enzymatic activity is required to promote adipocyte differentiation. To test if eLOX3 activity is required to induce adipocyte differentiation of $Rb^{-/-}$ MEFs, we constructed an enzymatically inactive eLOX3 mutant. Deletion of amino acids N155 to P195 (eLOX3Δ) abolished the enzymatic activity, as measured by the ability to convert 15(S)-HPETE into 13(R)-hydroxy-14(S),15(S)-HepEtrE (Fig. 2C). Whereas expression of full-length eLOX3 increased adipogenic conversion in $Rb^{-/-}$ MEFs, expression of eLOX3Δ in $Rb^{-/-}$ MEFs did not, as determined by oil red O staining and expression of PPARγ2 and aP2 (Fig. 2A and B). Furthermore, to elucidate whether eLOX3 activity was directly affected by baicalein, we tested the effect of increasing amounts of baicalein on the *in vitro* activity of eLOX3, as well as epidermal-type 12(S)-LOX (e12SLOX) and leukocyte-type 12(S)-LOX (l12SLOX). Addition of baicalein inhibited eLOX3 to a degree comparable to the inhibition of the two 12(S)-LOXs (Fig. 2D), suggesting that baicalein inhibits adipocyte differentiation by directly inhibiting eLOX3.

Hepoxilins promote adipocyte differentiation. eLOX3 converts HPETE intermediates into epoxyalcohol fatty acids in a hydroperoxide isomerase reaction. The 12-HPETE-derived epoxyalcohol fatty acids are known as hepoxilins (42, 63, 65). Hepoxilins are a group of epoxyalcohols derived from hydroperoxy fatty acids. Their function is best studied in relation to upholding the function of the epidermis. The group is normally segregated into two types of hepoxilins, A3 and B3, based on the distance between the epoxy and hydroxyl group. Hepoxilins of the A type are normally much more unstable than the B type hepoxilins. Type A hepoxilins are easily hydrolyzed either by acids or in cells by epoxide hydrolases and are therefore difficult to detect in biological extracts (8). To examine whether hepoxilin A3 or hepoxilin B3 could recapitulate the effects observed upon forced eLOX3 expression, we tested their ability to restore adipogenesis in the $Rb^{-/-}$ MEFs. $Rb^{-/-}$ MEFs were induced to differentiate according to the MDI protocol with the inclusion of 10 μM hepoxilin A3, hepoxilin B3, or vehicle control during the first 4 days of differentiation. Eight days after induction, cells were stained with oil red O (Fig. 2E), and RNA was harvested for analysis of expression of differentiation markers (Fig. 2F). Vehicle-treated cells did not differentiate, whereas inclusion of either hepoxilin A3 or B3 promoted adipocyte differentiation of the $Rb^{-/-}$ MEFs.

Forced expression eLOX3 induces adipose conversion of 3T3-L1 preadipocytes, and hepoxilins are produced during the initial stages of differentiation. Having established that eLOX3 can stimulate adipose conversion in $Rb^{-/-}$ MEFs, we sought to determine if eLOX3 also was able to induce adipocyte differentiation in 3T3-L1 preadipocytes. 3T3-L1 preadi-

of baicalein set to 100%. (E and F) Identified products of eLOX3, HXA3 and HXB3, increase adipose conversion of $Rb^{-/-}$ MEFs. Cells were induced to differentiate according to the MDI protocol with addition of 10 μM HXA3 or HXB3 or vehicle control at the time of induction and on days 1, 2, and 3. Adipogenic conversion was investigated 8 days after induction. (E) Morphological differentiation and staining of lipids by oil red O. (F) Expression of adipogenic marker genes by real-time PCR. PEPCK, phosphoenolpyruvate carboxykinase. One representative experiment out of three independent experiments performed in duplicate is shown.

pocytes readily undergo adipocyte differentiation when induced according to the MDI protocol, and an elevation of the cAMP level at the initiation of differentiation has been linked to the transient induction of PPARγ ligand production (54). The decrease in adipose conversion of 3T3-L1 preadipocytes by the exclusion of the cAMP-elevating compound can be circumvented by the inclusion of an exogenous PPARγ ligand. We therefore hypothesized that forced expression of eLOX3 could increase adipogenesis in 3T3-L1 preadipocytes induced with only dexamethasone and insulin. Indeed, ectopic expression of eLOX3 augmented adipocyte differentiation of 3T3-L1 preadipocytes (Fig. 3A). Furthermore, under the same conditions both hepoxilin A3 and B3 simulated adipose conversion of 3T3-L1 preadipocytes to a degree similar to rosiglitazone as assessed by oil red O and marker gene expression (Fig. 3B and C).

Tzameli and colleagues have shown that PPARγ ligand(s) is produced early and transiently during adipocyte differentiation in a cAMP-dependent manner, and the ligand(s) is detectable in the medium (54). We therefore examined conditioned medium from 3T3-L1 cells for the presence of hepoxilins during the early stages of the adipogenic conversion process using liquid chromatography tandem mass spectrometry (LC/MS/MS). By LC, hepoxilin A and hepoxilin B coeluted whether spiked with blank medium or not (data not shown). As ligand production was shown to be cAMP dependent, we analyzed conditioned medium from cells treated with DI or MDI for 24 h. Only lipids extracted from 3T3-L1 cells treated with MDI yielded substances with a chromatographic retention time compatible with the presence of hepoxilin A3 or B3 in the extract (Fig. 3D). The MS/MS fragmentation patterns of blank medium samples spiked with hepoxilin A3 or B3 are characterized by diagnostic fragment ions with m/z of 317, 299, 273, and 275, but it is possible at least partly to distinguish between the two by comparing the m/z 317 and 273 intensities. The intensity of fragment m/z 317 was higher than that of the m/z 273 fragment for hepoxilin B3 (ratio 317/273, $\sim$ 2.61), while the opposite was observed for hepoxilin A3 (ratio 317/273, $\sim$ 0.62). Furthermore, only fragmentation of hepoxilin B3 resulted in an ion with an m/z of 291. A similar pattern was observed when the pure compounds were analyzed. By MS/MS analysis of the sample derived from the MDI-treated sample, a fragmentation pattern clearly compatible with the presence of hepoxilins was observed. The presence of an ion with an m/z of 291 and the m/z 317/273 ratio of 2.63 suggests that at least hepoxilin B3 was generated during this early stage of the differentiation program, but the unstable nature of hepoxilin A3 makes it possible also that this hepoxilin is produced together with hepoxilin B3 (Fig. 3E). Moreover, consistent with the results of Tzameli and coworkers, the production of hepoxilin(s) was dependent on elevated cAMP levels.

Hepoxilins activate PPARγ. To test if hepoxilin A3 and B3 directly affected the activity of PPARγ, we transiently transfected $Rb^{-/-}$ MEFs with Gal4-DBD-PPARγ-LBD, a UAS-Gal-TK-luciferase reporter, and a CMV-β-galactosidase normalization vector and treated the cells with increasing amounts of hepoxilin A3 or B3. Figure 4A demonstrates that both hepoxilins activated PPARγ in a dose-dependent manner. At a concentration of 10 μM, the activation reached 40% of that observed with 0.5 μM rosiglitazone (Fig. 4A).

PPARδ has been shown to stimulate adipocyte differentiation (4, 5, 22, 36). Furthermore, retinoid X receptor α (RXRα) has been shown to bind fatty acids (14), and liganded RXR enhances the transactivating potential of the PPARγ/RXR heterodimer (51). Therefore, we examined whether the hepoxilins activated PPARδ or RXRα using transient transfection of $Rb^{-/-}$ MEFs with Gal4-DBD-PPARδ-LBD or Gal4-DBD-RXRα-LBD as described above. Neither hepoxilin A3 nor hepoxilin B3 activated RXRα, and they only very weakly activated PPARδ, suggesting that the adipogenic effect of hepoxilins is not mediated via activation of PPARδ or RXRα (data not shown). In addition, Gal4-DBD-PPARα-LBD was not activated by either hepoxilin A3 or B3 in $Rb^{-/-}$ MEFs (data not shown). To further test whether hepoxilin A3 or B3 bound directly to PPARγ through its ligand binding pocket, we determined their relative binding affinities in a ligand displacement assay (Fig. 4B). Both hepoxilins displaced the binding of fluorescent ligand to PPARγ with 50% K_d (K_d50) values for rosiglitazone, hepoxilin A3, and hepoxilin B of 27 nM, 11 μM, and 4 μM, respectively. The apparently high K_d50 value for the hepoxilins may reflect the inherent instability of the epoxide ring in these compounds in aqueous solution. However, collectively our results indicate that the effects observed on both activation of PPARγ and adipocyte differentiation could be mediated through direct binding to the PPARγ LBD.

Hypothetically, hepoxilins might augment PPARγ-mediated transactivation in a manner independent of binding to the ligand binding domain. To examine this possibility, we took advantage of a PPARγ mutant (PPARγ Q286P) in which a glutamine-to-proline exchange of residue 286 abolishes the ability of PPARγ to bind and become activated by virtually all known ligands (48, 55). Figure 4C shows that hepoxilin A3 and B3 increased the activity of wild-type PPARγ, whereas both hepoxilins failed to augment the activity of PPARγ Q286P, supporting the notion that hepoxilins activate PPARγ by binding to the ligand binding domain and thereby activating the AF2 function.

Synthetic PPARγ agonists have been widely used clinically because of their ability to increase insulin sensitivity. We therefore examined if the hepoxilins could increase insulin signaling in differentiated 3T3-L1 adipocytes by measuring insulin-dependent glucose uptake. Both hepoxilin A3 and B3 potentiated insulin-stimulated glucose uptake to levels similar to rosiglitazone (Fig. 4D). Neither the two hepoxilins nor rosiglitazone affected the protein levels of the two glucose-transporters, GLUT1 and GLUT4 (see Fig. S2 in the supplemental material).

PPARγ agonists increase transactivation by facilitating binding of coactivators. TRAP220 (Mediator Subunit 1, Med1) can be directly recruited to PPARγ in a ligand-dependent manner and is part of the mediator complex shown to be required for adipogenesis (18, 19). Furthermore, full PPARγ agonists have been shown to recruit TRAP220 more efficiently than partial PPARγ agonists (37). We therefore examined the ability of hepoxilins to enhance binding of TRAP220 to PPARγ. Hepoxilin B3 enhanced binding of TRAP220 to the PPARγ LBD to a level comparable to that of rosiglitazone, whereas recruitment mediated by hepoxilin A3 was lower (Fig. 4E). The low level of recruitment of TRAP220 in response to hepoxilin A3 may at least in part be due to the highly unstable nature of
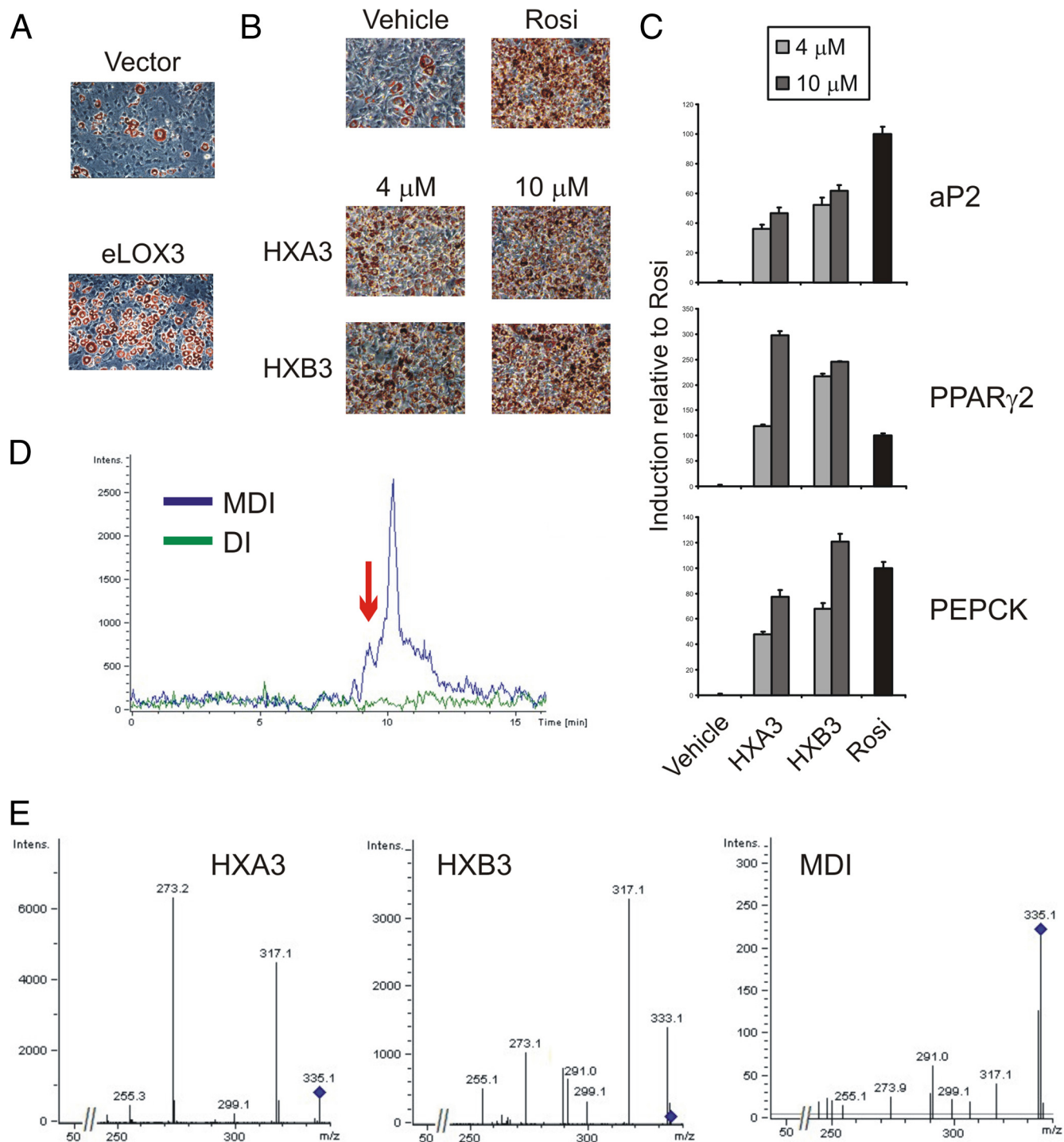
FIG. 3. eLOX3 and its products induce adipogenesis in 3T3-L1 preadipocytes. Cells were transduced with either empty vector or eLOX3-expressing vector and selected using puromycin. Cells were induced to differentiate with dexamethasone and insulin. Eight days after induction, cells were scored for differentiation as measured by oil red O staining (A). (B and C) 3T3-L1 cells were induced to differentiate with dexamethasone and insulin and with addition of HXA3, HXB3, rosiglitazone, or vehicle control at the time of induction and on days 1, 2, and 3. Adipogenic conversion was investigated 8 days after induction. (B) Morphological differentiation and staining of lipids by oil red O. (C) Expression of adipogenic marker genes by real-time PCR. Data are represented as induction relative to the induction by rosiglitazone over vehicle control. Induction by rosiglitazone is set to 100%. PEPCK, phosphoenolpyruvate carboxykinase. (D) LC/MS analyses of conditioned medium samples from 3T3-L1 cells treated with either DI or MDI for 24 h. Only peaks from signals corresponding to species with a molecular mass similar to that of hepoxilin (335.1 Da) are shown. The peak from the eluted hepoxilin is marked by a red arrow. (E) MS/MS analyses of hepoxilin standards (left and middle panels) and the coeluting peak from day 1 medium from 3T3-L1 cells induced to differentiate with MDI. One representative experiment out of two independent experiments performed in duplicate is shown.
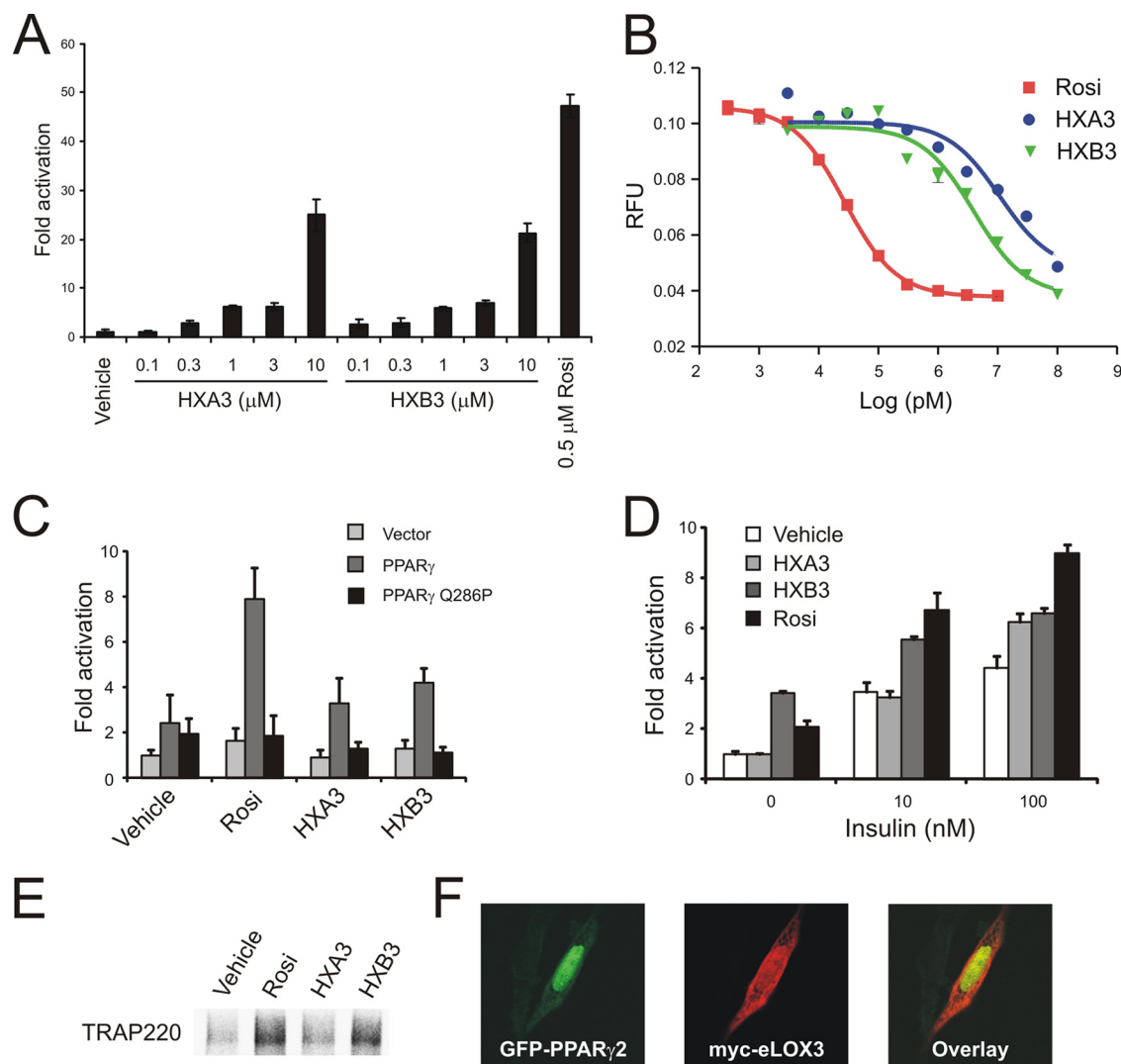
FIG. 4. Hepoxilin A3 and B3 bind and activate PPARγ. (A) HXA3 and HXB3 activate PPARγLBD in a dose-dependent manner. $Rb^{-/-}$ MEFs transfected with a Gal4-DBD-PPARγ-LBD expression vector and a UASGal-TK-luciferase reporter were treated with vehicle, 0.5 μM rosiglitazone, or increasing concentrations of HXA3 or HXB3. Luciferase activity was normalized to ß-galactosidase activity and is presented as fold change over vehicle only control. One representative experiment out of four independent experiments performed in triplicate is shown. (B) HXA3, HXB3, and rosiglitazone displace a fluorescent ligand from the PPARγ-LBD. RFU, relative fluorescence units. One representative experiment out of three independent experiments performed in triplicate is shown. (C) $Rb^{-/-}$ MEFs transfected with pDR1 Luc and either PPARγ, PPARγ Q286P, or empty vector treated with 1 μM rosiglitazone, 10 μM HXA3, or 10 μM HXB3. Luciferase activity was normalized to β-galactosidase activity. Data represent three independent experiments performed in triplicate. (D) Potentiation of insulin-stimulated glucose uptake by vehicle, rosiglitazone, HXA3, or HXB3. Differentiated 3T3-L1s were treated with the indicated compounds, and basal or insulin-stimulated uptake of radioactively labeled glucose was measured. Data are presented as fold uptake over the vehicle only control. Data represent two independent experiments performed in octuplicate. (E) GST-PPARγ DE pulldown of TRAP220 in the presence of vehicle, 1 μM rosiglitazone, 10 μM HXA3, or 10 μM HXB3. One representative experiment out of two independent experiments is shown. (F) 3T3-L1 cells were transfected with GFP-PPARγ2 and myc-eLOX3, and localization of the two fusion proteins was determined by confocal microscopy.

hepoxilin A3. To examine in more detail the ability of hepoxilins to recruit cofactors to PPARγ, we attempted to use a microarray approach to determine interactions between PPARγ and peptides derived from 18 known coregulators (31). However, incompatibility between hepoxilins and dithiothreitol (DTT) needed in the buffers for this assay prevented acquisition of consistent data (results not shown).

As an alternative method to examine the possible binding of hepoxilin A3 and B3 to PPARγ, the putative binding modes of both compounds were determined by docking into the ligand-binding pocket (see Fig. S3 in the supplemental material). Schwabe and colleagues recently showed that two molecules of 9-HODE, which is structurally similar to hepoxilin A3 and B3, bind simultaneously to the PPARγ ligand-binding pocket (24). When two molecules of either hepoxilin A3 and B3 were docked to the PPARγ ligand-binding pocket, ligand-protein interactions similar to the binding mode of 9-HODE were observed. Therefore, we hypothesized that two molecules of the hepoxilins could bind simultaneously to PPARγ. Based on this assumption, the putative binding mode of hepoxilin A3

included three hydrogen bonds formed between the oxygen atoms of the carboxylic acid group of the first molecule of hepoxilin A3 and Ser289, His449, and Tyr473 as well as one hydrogen bond located between the hydroxyl moiety of the second hepoxilin A3 and Glu295. In addition, the hydroxyl moiety of the first hepoxilin A3 molecule is involved in hydrogen bonds with one of the carboxyl oxygens of the second hepoxilin A3 as well as with the epoxy oxygen of the same molecule. Moreover, the hepoxilin A3 molecule that formed hydrogen bonds to the active site residues Ser289, His449, and Tyr473 established hydrophobic contacts to residues Ala278, Ile281, Leu356, and Phe360, whereas the second molecule exhibited hydrophobic interactions with residue Ile341.

The best docking pose for hepoxilin B3 had two hydrogen bonds between the oxygen atoms of the carboxylic acid moiety of the first hepoxilin B3 and residues His449 and Tyr473 and another hydrogen bond between the hydroxyl moiety of this ligand and residue Ser289. The second hepoxilin B3 molecule forms one hydrogen bond between its hydroxyl moiety and Glu295. Furthermore, one hydrogen bond was established between the hydroxyl moiety of the first hepoxilin B3 and one carboxyl oxygen of the second hepoxilin B3 molecule. Finally, the hepoxilin B3 molecule predicted to bind to the active site residues Ser289, His449, and Tyr473 exhibited hydrophobic interactions with residues Leu330, Val339, Ile341, and Met364, whereas the second hepoxilin B3 molecule was involved in a hydrophobic interaction with residue Ile262.

Spatial uncoupling of the site of production of a signaling molecule and the mediator could pose a problem for the conduction of a signal, especially for compounds containing structures as unstable as the epoxide ring in hepoxilins. We therefore examined the localization of eLOX3 and PPARγ in 3T3-L1 preadipocytes. As can be seen in Fig. 4F, PPARγ localized solely to the nucleus, whereas eLOX3 was present both in the cytoplasm and the nucleus. Its presence in the nucleus near PPARγ indicates that hepoxilin could be generated close to PPARγ, leading to local concentrations sufficient to activate the nuclear receptor.

Downregulation of eLOX3 in 3T3-L1 blocks adipocyte differentiation. As eLOX3 has a stimulatory effect on adipogenesis, we speculated if eLOX3 was required for adipocyte differentiation of 3T3-L1 preadipocytes. We therefore knocked down expression of eLOX3 in 3T3-L1 cells and measured their ability to undergo adipose conversion. Cells were transduced with five different short hairpin RNA (shRNA)-expressing vectors specifically designed to silence eLOX3 or an empty vector control. Pools of selected cells were seeded and either harvested for analysis of eLOX3 expression (day 0) or induced to differentiate according to the standard MDI protocol. Six days after induction, cells were Oil red O stained, and protein was harvested for analysis of differentiation markers (Fig. 5A and B). Three shRNA constructs, sheLOX3-1, sheLOX3-2, and sheLOX3-3, reduced eLOX3 expression below the limit of detection on day 0 (Fig. 5B). On day 6, expression of eLOX3 had been partially restored in cells transduced with sheLOX3-1, whereas eLOX3 expression was still significantly suppressed in cells transduced with sheLOX3-2 and sheLOX3-3. Of note is the striking inverse relationship between eLOX3 expression on day 6 and adipocyte differentiation. eLOX3 expression was most efficiently repressed in

cells transduced with sheLOX3-2 and sheLOX3-3, and these cells did not differentiate, as measured by oil red O staining and expression of the adipocyte markers, aP2 and PPARγ. Slight expression of eLOX3 in sheLOX3-1-transfected cells correlated with expression of PPARγ and aP2.

As an alternative for downregulation of eLOX3 expression, we next employed RNAi as a tool to knock down eLOX3 expression. As seen in Fig. 5C and D, eLOX3 silencing by RNAi partly recapitulated the phenotype observed by shRNA silencing of eLOX3. We assume that the observed differences in degree of suppression of adipocyte differentiation relate to differences in the efficiency of RNAi transfection versus retroviral transduction and selection. Importantly, however, the impaired adipogenic conversion observed by eLOX3 silencing could be bypassed by adding rosiglitazone during differentiation, as visualized by oil red O staining (Fig. 5C), and expression of phosphoenolpyruvate carboxykinase (PEPCK), an adipocyte marker (Fig. 5D).

XOR and eLOX3 synergistically enhance PPARγ-mediated transactivation. As described above, eLOX3 cannot by itself use arachidonic acid as a substrate but can catalyze only the conversion of HPETEs into epoxyalcohols. HPETEs are normally considered to be generated solely by other LOXs. This makes eLOX3 a counterintuitive candidate for PPARγ agonist production as no other LOXs are present at detectable levels in 3T3-L1 cells (35). Still, we observed increased levels of HETEs, the degradation products of HPETEs, upon induction of differentiation (Fig. 6A). The dioxygenation catalyzed by LOXs resembles that of lipid auto-oxidation, suggesting that the presence of ROS during adipocyte differentiation could result in generation of HPETEs. Recently, XOR was shown to be implicated in the production of PPARγ ligands during adipogenesis (13), and blocking the ROS-generating site of XOR abolished ligand production. We therefore hypothesized that XOR could generate HPETEs through ROS formation, thereby cooperating with eLOX3 in the production of PPARγ-activating hepoxilins. Auto-oxidation of arachidonic acid by ROS results in the generation of isoprostanes, malondialdehydes, 4-hydroxy-nonenals, and HPETEs (40), of which the latter can be converted into hepoxilins by eLOX3.

To test the effect of XOR and eLOX3 on PPARγ activation, we examined the transactivating activity of Gal4-DBD-PPARγ-LBD in the presence of either XOR, eLOX3, or both (Fig. 6B). Interestingly, in the presence of low concentrations of arachidonic acid (5 μM), XOR or eLOX3 alone minimally increased the activity of the PPARγ-LBD. However, when both were expressed, PPARγ-mediated transactivation was synergistically enhanced. Even though hepoxilins efficiently restored adipogenesis in the $Rb^{-/-}$ MEFs (Fig. 2), forced expression of eLOX3 resulted in only a modest rescue of adipocyte differentiation (Fig. 1 and 2), suggesting that the generation of eLOX3 substrates is diminished in the $Rb^{-/-}$ MEFs. Indeed, these MEFs fail to induce expression of XOR upon administration of the differentiation cocktail (Fig. 6C). It was, however, impossible to examine a synergistic effect of eLOX3 and XOR on adipocyte differentiation as forced expression of XOR blocks adipogenesis (13). Collectively, these data suggest that eLOX3 and XOR cooperate in the activation of PPARγ during the early stages of adipocyte differentiation.
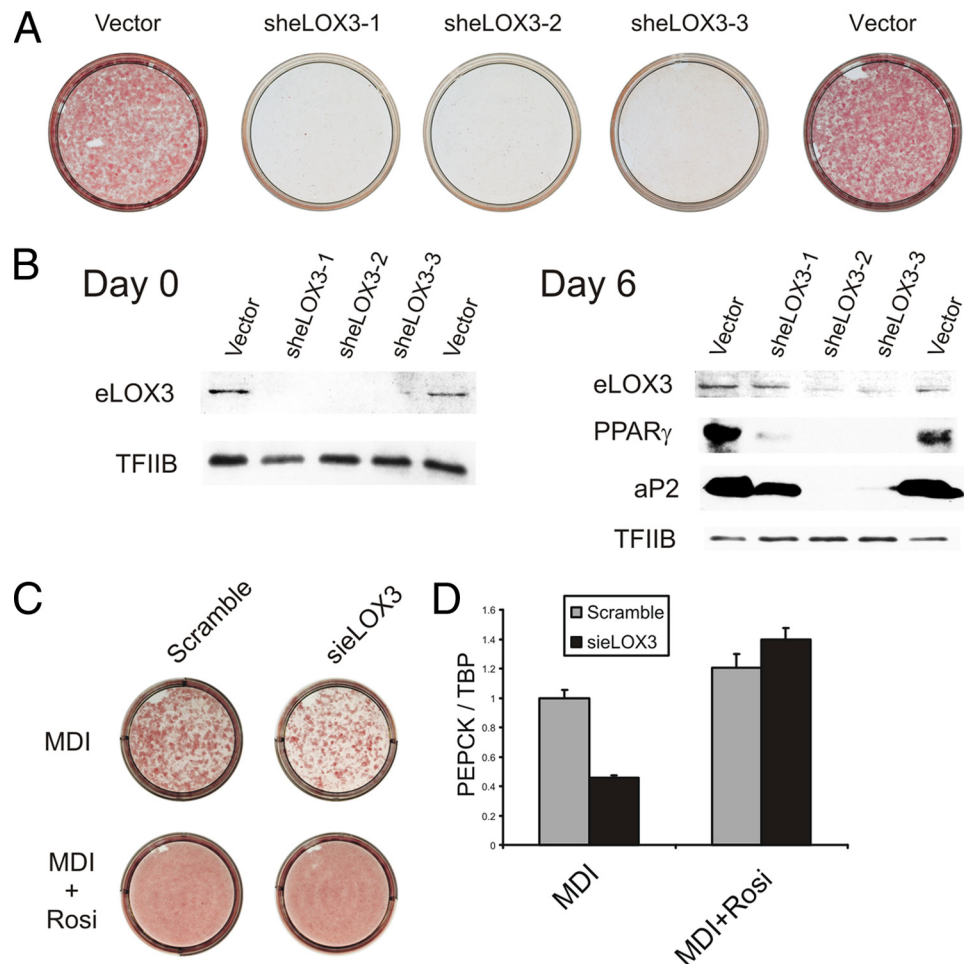
FIG. 5. Knockdown of eLOX3 expression prevents adipocyte differentiation of 3T3-L1 cells. Cells were transduced with shRNA constructs against eLOX3, selected with puromycin, and induced to differentiate according to the MDI protocol. (A) Cells stained with oil red O. (B) Detection of eLOX3 expression and adipocyte markers using Western blotting. TFIIB was included as a loading control. One representative experiment out of three independent experiments performed in duplicate is shown. (C and D) 3T3-L1 preadipocytes were transfected with either scrambled or eLOX3 RNAi using DeliverX Plus and induced to differentiate in the presence or absence of 0.5 μM rosiglitazone. (C) Cells were stained for lipid accumulation using oil red O. (D) Expression of PEPCK mRNA as a marker for differentiation was examined by real-time PCR. One representative experiment out of two independent experiments performed in triplicate is shown.

The antioxidant *N*-acetyl cysteine (NAC) inhibits adipose conversion. If the generation of PPARγ ligand(s) involved a ROS-mediated conversion of arachidonic acid into eLOX3 substrates, we hypothesized that scavenging ROS using an antioxidant compound would have an antiadipogenic effect. NAC is commonly used as a tool to remove ROS. As predicted, NAC abolished adipose conversion of 3T3-L1 preadipocytes as measured by oil red O and marker gene expression (Fig. 7A and B). Furthermore, the NAC-mediated inhibition was circumvented by the inclusion of an exogenous PPARγ ligand during differentiation. The decline in PPARγ mRNA levels by rosiglitazone was expected based on previous reports (11, 47). As PPARγ ligand(s) is produced early and transiently during adipocyte differentiation, NAC should be required early in order to abolish adipogenesis. Indeed, inclusion of NAC from day 0 to day 4 was sufficient to inhibit adipocyte differentiation (Fig. 7C and D). Furthermore, addition of NAC from day 2 onwards resulted in a modest inhibition, whereas inclusion from day 4 or day 6 to the end of differentiation had no effect

on adipose conversion (data not shown). Collectively, these data indicate a requirement for early production of ROS for induction of adipocyte differentiation. Interestingly, the level of ROS was recently shown to increase during the early stages of adipocyte differentiation. It was suggested that ROS was important for activation of C/EBPβ and that antioxidants inhibited adipogenesis by blocking activation of C/EBPβ (32). However, the inclusion of the antioxidant NAC in the differentiation cocktail reduced C/EBPβ mRNA expression only marginally and augmented rather than inhibited induction of the C/EBPβ-responsive gene XOR (Fig. 7E), suggesting that ROS-dependent effects on C/EBPβ activity do not affect XOR expression.

DISCUSSION

The role of PPARγ in adipocyte differentiation is well established (3, 45). However, the identity of the endogenous PPARγ ligand(s) promoting the early stages of adipocyte dif-
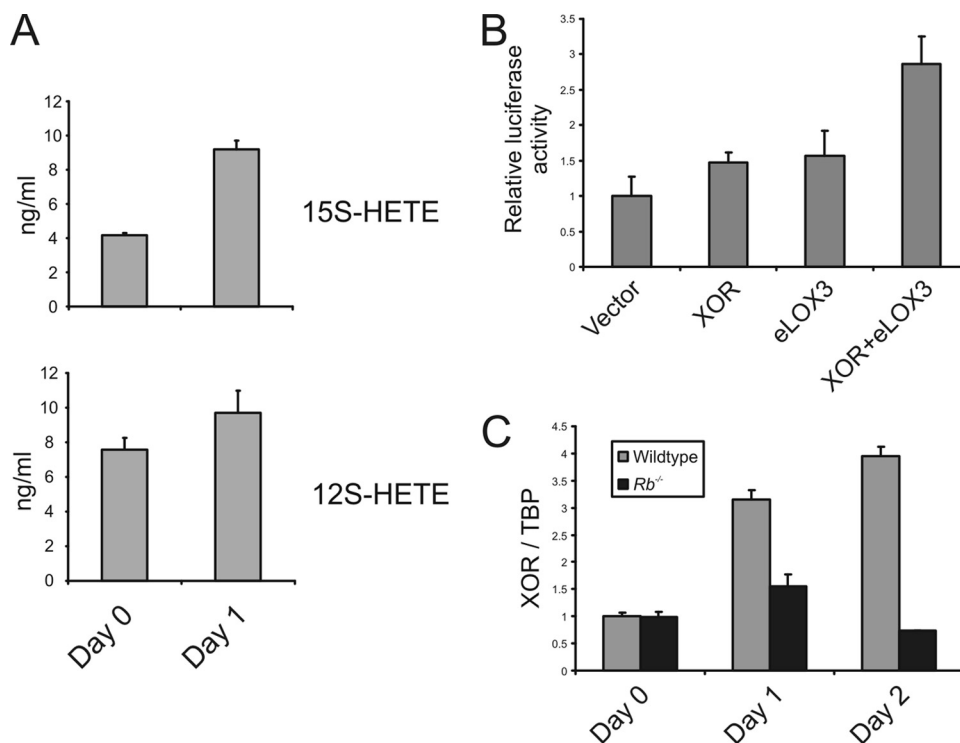
FIG. 6. eLOX3 cooperates with XOR in the activation of PPARγ. (A) 15(S)- and 12(S)-HETE in the medium from wild-type MEFs before (day 0) and 24 h after (day 1) induction with MDI. Data represent two independent experiments performed in duplicate. (B) $Rb^{-/-}$ MEFs were transiently transfected using UASGal-TK-luciferase reporter, Gal4-DBD-PPARγ-LBD, and either XOR, eLOX3, or both. Transfected cells were stimulated with 5 μM arachidonic acid. Luciferase activity was normalized to ß-galactosidase activity and is presented as fold change over vector only control. One representative experiment out of four independent experiments performed in triplicates is shown. (C) Expression of XOR in wild-type and $Rb^{-/-}$ MEFs was analyzed by real-time PCR and normalized to TBP expression. Data represent two independent experiments performed in triplicate.

ferentiation has so far remained elusive. Earlier studies identified prostaglandins as potential endogenous agonists promoting adipocyte differentiation. The naturally occurring 15-dPGJ$_2$ has been shown to activate PPARγ and promote adipocyte differentiation (17, 28). However, evidence has been presented arguing that 15-dPGJ$_2$ is not a bona fide endogenous agonist during adipocyte differentiation (6, 43, 54).

Nitrolinoleic acid (LNO$_2$) is another naturally occurring potent activator of PPARγ and a strong inducer of adipocyte differentiation (50). The majority of LNO$_2$ in tissues is esterified and embedded in the cell membranes. Although esterified LNO$_2$ is present in quantities sufficient to support PPARγ activation (2, 50), no direct assessment of release of LNO$_2$ during adipogenesis has been reported.

The role of LOXs as generators of endogenous adipogenic PPARγ agonists has been a matter of dispute. We previously showed that adipocyte differentiation of the 3T3-L1 preadipocyte is inhibited by the LOX inhibitor baicalein and that this inhibition was rescued by the addition of rosiglitazone. Moreover, we presented evidence that the activation of a PPARγ-LBD reporter during adipogenesis was sensitive to baicalein (35). Using a stably integrated PPARγ ligand-sensing reporter system in 3T3-L1 cells, Tzameli et al. reported that treatment with baicalein during adipose conversion did not prevent activation of the reporter and concluded that LOXs were not involved in the production of endogenous PPARγ agonist in

these cells (54). However, this study did not report if treatment with baicalein abolished adipocyte differentiation. Baicalein is very unstable in aqueous solution (39), and auto-oxidation changes its characteristics (67). The low stability, sensitivity to oxidation, and the fact that the mere presence of baicalein in the medium leads to activation of a PPARγ ligand-sensing reporter (35) could lead to an erroneous conclusion regarding the importance of LOXs in the generation of endogenous adipogenic PPARγ agonists.

ADD1 has been linked to the generation of PPARγ ligand(s). Here, we show that ADD1 is able to restore adipogenesis in $Rb^{-/-}$ MEFs in a LOX-dependent manner through induction of eLOX3 and p12SLOX expression. However, several observations indicate that this ADD1-eLOX3/p12SLOX pathway is not involved in PPARγ ligand production during normal adipocyte differentiation of 3T3-L1 cells. First, no expression of p12SLOX can be detected in 3T3-L1 cells, and eLOX3 is the only LOX detectable in differentiating 3T3-L1 preadipocytes (35). Second, generation of PPARγ ligand(s) during adipocyte differentiation relies on the cAMP-elevating compound in the hormonal cocktail used to induce adipogenic conversion (54), and several groups have reported an inhibition of SREBP maturation and activity by cAMP (34, 58, 66). Thus, our results suggest that the ADD1-dependent induction of adipocyte differentiation and PPARγ ligand production is an artifact of forced ADD1 expression.
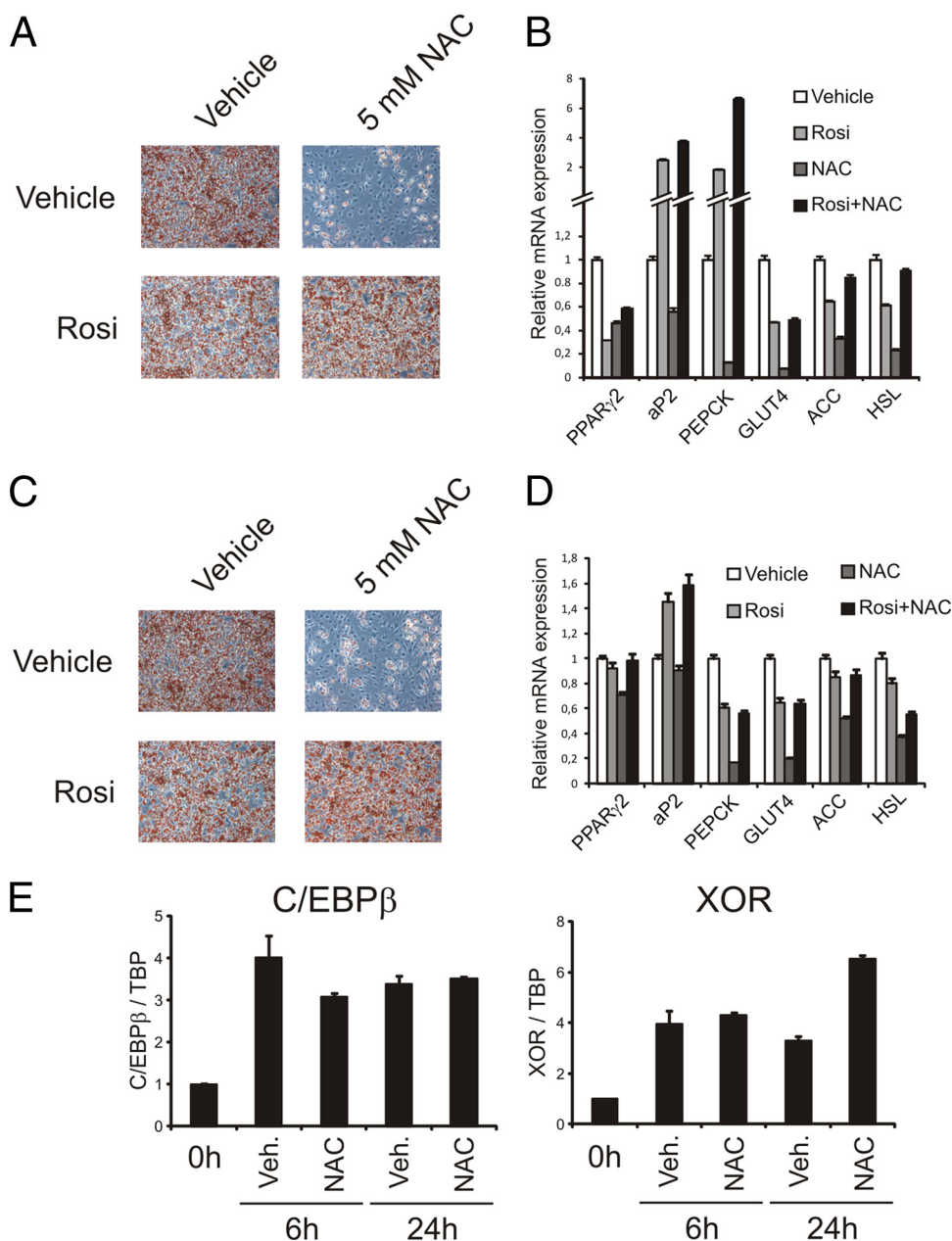
FIG. 7. The antioxidant NAC abolishes adipose conversion. (A and B) 3T3-L1 preadipocytes were induced to differentiate according to the MDI protocol with the inclusion of rosiglitazone (0.5 μM) and/or NAC (5 mM) or vehicle alone. Differentiation was determined by oil red O staining (A) or expression of adipocyte marker genes (B). ACC, acetyl coenzyme A carboxylase; HSL, hormone-sensitive lipase; GLUT4, facilitated glucose transporter, member 4. Data represent two independent experiments performed in duplicate. (C and D) 3T3-L1 preadipocytes were induced to differentiate according to the MDI protocol with the inclusion of rosiglitazone (0.5 μM) and/or NAC (5 mM) or vehicle alone from day 0 to day 4. Differentiation was determined by oil red O staining (C) and expression of adipocyte marker genes (D). Data represent two independent experiments performed in duplicate. (E) 3T3-L1 cells were induced to differentiate in the presence and absence of 5 mM NAC. Expression of C/EBPβ and XOR was analyzed at indicated time points. Data represent two independent experiments performed in duplicate.

In contrast to other LOXs, eLOX3 functions as a hydroperoxide isomerase converting dioxygenated fatty acids into hepoxilins (63, 65). The absence of others LOXs in 3T3-L1 cells, however, makes eLOX3 a counterintuitive candidate for production of a PPARγ ligand during adipogenesis. Recently, Cheung and coworkers demonstrated the requirement for XOR, a potent generator of ROS, for the production of ligand(s) during adipocyte differentiation (13). Of note, LOXs

catalyze dioxygenation of fatty acids in a stereo- and site-specific manner, but this reaction is chemically equivalent to hydrocarbon auto-oxidation by ROS (49, 59). In keeping with the finding that XOR and eLOX3 cooperated in the activation of a Gal4-DBD-PPARγ-LBD fusion protein, this strongly suggests that ROS produced by XOR generate dioxygenated fatty acids through auto-oxidation, thereby creating substrates for eLOX3. This is further strengthened by our finding that the

inclusion of a ROS-scavenger, NAC, inhibited adipose conversion.

Hepoxilins fall into two types, A and B. The lower stability of the A type could explain our observed lower affinity for binding to the PPARγ-LBD (Fig. 4B) and the apparent low recovery of hepoxilin A in the conditioned medium (Fig. 3D). It is likely that both hepoxilins are produced during differentiation as ROS-mediated auto-oxidation of arachidonic acid presumably would lead to the generation of precursors for both hepoxilin A3 and B3.

Both hepoxilins have a relatively low affinity for PPARγ (K_d50 values at 11 and 4 μM for hepoxilin A3 and hepoxilin B3, respectively). Such high concentrations are unlikely to be found in crude biological extracts. However, the local concentration at the site of production within the cell may be much higher. In that respect, it is noteworthy that eLOX3 at least in part colocalizes with PPARγ in 3T3-L1 preadipocytes, suggesting that locally produced hepoxilins may be channeled to PPARγ (Fig. 4D).

Recently, Yu and colleagues reported that a hepoxilin of the A type was able to activate PPARα but neither of the other PPARs (64). These analyses, however, were done in keratinocytes which are high in epoxide hydrolase activity, and the degradation product of the hepoxilin was as potent as the hepoxilin in activating PPARα. It is therefore possible that it is the degradation product that is the true ligand for PPARα, and differences in epoxide hydrolase activity between keratinocytes and MEFs could explain the discrepancies between our findings.

Data presented here suggest that pRB is involved in the expression of both XOR and eLOX3. Although eLOX3 mRNA expression drops at the onset of differentiation, the protein level remains relatively stable during early stages of differentiation (35). pRB appears to be involved in the regulation of expression of eLOX3 as $Rb^{-/-}$ MEFs have lower levels of eLOX3 protein than wild-type MEFs. Furthermore, the $Rb^{-/-}$ MEFs fail to increase XOR expression upon induction of differentiation. This effect is most likely mediated through C/EBPβ, as this transcription factor is required for induction of XOR (13), and pRB has previously been shown to cooperate with C/EBPβ during adipocyte differentiation (12). Taken together, our results suggest a pathway in which XOR and eLOX3 cooperate in the generation of PPARγ activators, where pRB is involved in the regulation of expression of the two enzymes. Possible pathways involved in the generation of hepoxilins during the initial stages of adipocyte differentiation are depicted in Fig. 8.

Walkey and Spiegelman recently expressed a mutated PPARγ, virtually devoid of ligand-binding ability, in PPARγ-deficient MEFs and found that under these specific circumstances, ligand binding/activation was dispensable for adipogenesis. However, an intact ligand-dependent transactivating function (AF-2) of PPARγ was required (55). A way to reconcile this result with our notion that ligand production is necessary for the initiation of adipocyte differentiation would be that a ligand-dependent activation of AF-2 occurs early during the adipogenic program when expression of PPARγ is at its lowest. The presence of ligands becomes dispensable after PPARγ has accumulated to the high levels observed in mature adipocytes. Thus, forced expression of a ligand-bind-
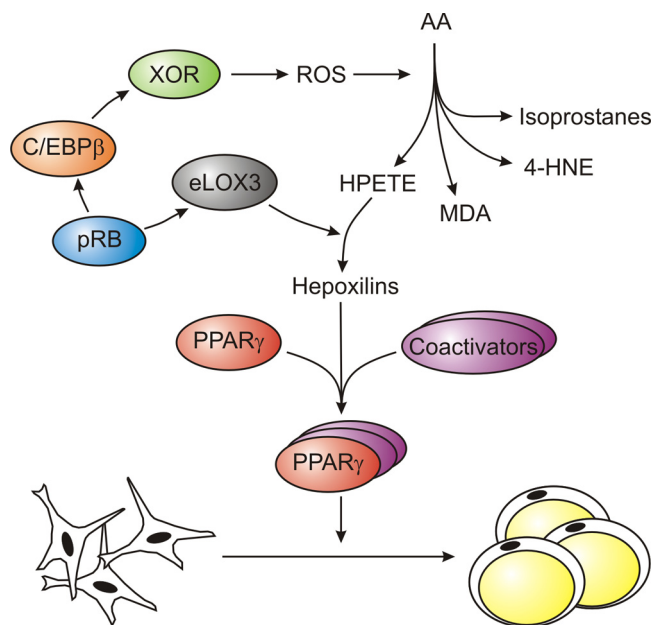

FIG. 8. Hypothetical pathway for the generation of PPARγ ligands during the early stages of adipocyte differentiation. AA, arachidonic acid; MDA, malondialdehyde; 4-HNE, 4-hydroxy-nonenals.

ing-deficient but active PPARγ at the onset of adipogenesis would presumably circumvent the requirement for a ligand-mediated activation of PPARγ during the early stage of adipose conversion.

In conclusion, our findings indicate that hepoxilins are produced by the synergistic action of XOR and the unconventional eLOX3. This group of oxidized fatty acids can function as PPARγ activators, and several lines of evidence presented here show that the hepoxilins possess a number of characteristics compatible with the idea that hepoxilins may constitute endogenous PPARγ agonists that contribute to PPARγ activation during the initiation of adipocyte differentiation. Whereas the importance of eLOX3 for adipocyte differentiation *in vitro* has been clearly demonstrated, it is conceivable that other pathways may also control the initiation and production of PPARγ agonist *in vivo*. Whereas eLOX3 is the sole LOX expressed in detectable amounts in 3T3-L1 (35) and 3T3-F442A (data not shown) preadipocyte cell lines, several other LOXs are expressed in adipose tissues (35). Thus, further experiments are clearly needed in order to establish the biological significance of eLOX3 and hepoxilins in the activation of PPARγ *in vivo*.

REFERENCES

1. **Araujo, P., Z.-Y. Du, T.-T. Nguyen, and E. Holen.** 2008. Direct injection of redissolved cell culture media into a single-column liquid chromatography

coupled to mass spectrometry for the measurement of PGE2. Open Anal. Chem. J. **2:**62–66.

2. **Baker, P. R., F. J. Schopfer, S. Sweeney, and B. A. Freeman.** 2004. Red cell membrane and plasma linoleic acid nitration products: synthesis, clinical identification, and quantitation. Proc. Natl. Acad. Sci. U. S. A. **101:**11577–11582.

3. **Barak, Y., M. C. Nelson, E. S. Ong, Y. Z. Jones, P. Ruiz-Lozano, K. R. Chien, A. Koder, and R. M. Evans.** 1999. PPAR gamma is required for placental, cardiac, and adipose tissue development. Mol. Cell **4:**585–595.

4. **Bastie, C., D. Holst, D. Gaillard, C. Jehl-Pietri, and P. A. Grimaldi.** 1999. Expression of peroxisome proliferator-activated receptor PPARdelta promotes induction of PPARγ and adipocyte differentiation in 3T3C2 fibroblasts. J. Biol. Chem. **274:**21920–21925.

5. **Bastie, C., S. Luquet, D. Holst, C. Jehl-Pietri, and P. A. Grimaldi.** 2000. Alterations of peroxisome proliferator-activated receptor delta activity affect fatty acid-controlled adipose differentiation. J. Biol. Chem. **275:** 38768–38773.

6. **Bell-Parikh, L. C., T. Ide, J. A. Lawson, P. McNamara, M. Reilly, and G. A. FitzGerald.** 2003. Biosynthesis of 15-deoxy-delta12,14-PGJ2 and the ligation of PPARγ. J. Clin. Invest. **112:**945–955.

7. **Berman, H. M., J. Westbrook, Z. Feng, G. Gilliland, T. N. Bhat, H. Weissig, I. N. Shindyalov, and P. E. Bourne.** 2000. The Protein Data Bank. Nucleic Acids Res. **28:**235–242.

8. **Brash, A. R., Z. Yu, W. E. Boeglin, and C. Schneider.** 2007. The hepoxilin connection in the epidermis. FEBS J. **274:**3494–3502.

9. **Burger, F., P. Krieg, F. Marks, and G. Furstenberger.** 2000. Positional- and stereo-selectivity of fatty acid oxygenation catalysed by mouse (12S)-lipoxygenase isoenzymes. Biochem. J. **348:**329–335.

10. **Camp, H. S., A. Chaudhry, and T. Leff.** 2001. A novel potent antagonist of peroxisome proliferator-activated receptor gamma blocks adipocyte differentiation but does not revert the phenotype of terminally differentiated adipocytes. Endocrinology **142:**3207–3213.

11. **Camp, H. S., A. L. Whitton, and S. R. Tafuri.** 1999. PPARgamma activators down-regulate the expression of PPARγ in 3T3-L1 adipocytes. FEBS Lett. **447:**186–190.

12. **Chen, P. L., D. J. Riley, Y. Chen, and W. H. Lee.** 1996. Retinoblastoma protein positively regulates terminal adipocyte differentiation through direct interaction with C/EBPs. Genes Dev. **10:**2794–2804.

13. **Cheung, K. J., I. Tzameli, P. Pissios, I. Rovira, O. Gavrilova, T. Ohtsubo, Z. Chen, T. Finkel, J. S. Flier, and J. M. Friedman.** 2007. Xanthine oxidoreductase is a regulator of adipogenesis and PPARγ activity. Cell Metab. **5:**115–128.

14. **de Urquiza, A. M., S. Liu, M. Sjoberg, R. H. Zetterstrom, W. Griffiths, J. Sjovall, and T. Perlmann.** 2000. Docosahexaenoic acid, a ligand for the retinoid X receptor in mouse brain. Science **290:**2140–2144.

15. **Fajas, L., V. Egler, R. Reiter, J. Hansen, K. Kristiansen, M. B. Debril, S. Miard, and J. Auwerx.** 2002. The retinoblastoma-histone deacetylase 3 complex inhibits PPARγ and adipocyte differentiation. Dev. Cell **3:**903–910.

16. **Farmer, S. R.** 2006. Transcriptional control of adipocyte formation. Cell Metab. **4:**263–273.

17. **Forman, B. M., P. Tontonoz, J. Chen, R. P. Brun, B. M. Spiegelman, and R. M. Evans.** 1995. 15-Deoxy-$\Delta^{12,14}$-prostaglandin J_2 is a ligand for the adipocyte determination factor PPARγ. Cell **83:**803–812.

18. **Ge, K., Y. W. Cho, H. Guo, T. B. Hong, M. Guermah, M. Ito, H. Yu, M. Kalkum, and R. G. Roeder.** 2008. Alternative mechanisms by which mediator subunit MED1/TRAP220 regulates peroxisome proliferator-activated receptor gamma-stimulated adipogenesis and target gene expression. Mol. Cell. Biol. **28:**1081–1091.

19. **Ge, K., M. Guermah, C. X. Yuan, M. Ito, A. E. Wallberg, B. M. Spiegelman, and R. G. Roeder.** 2002. Transcription coactivator TRAP220 is required for PPAR gamma 2-stimulated adipogenesis. Nature **417:**563–567.

20. **Hamm, J. K., B. H. Park, and S. R. Farmer.** 2001. A role for C/EBPβ in regulating peroxisome proliferator-activated receptor gamma activity during adipogenesis in 3T3-L1 preadipocytes. J. Biol. Chem. **276:**18464–18471.

21. **Hansen, J. B., R. K. Petersen, B. M. Larsen, J. Bartkova, J. Alsner, and K. Kristiansen.** 1999. Activation of peroxisome proliferator-activated receptor gamma bypasses the function of the retinoblastoma protein in adipocyte differentiation. J. Biol. Chem. **274:**2386–2393.

22. **Hansen, J. B., H. Zhang, T. H. Rasmussen, R. K. Petersen, E. N. Flindt, and K. Kristiansen.** 2001. Peroxisome proliferator-activated receptor delta (PPARδ)-mediated regulation of preadipocyte proliferation and gene expression is dependent on cAMP signaling. J. Biol. Chem. **276:**3175–3182.

23. **Huang, J. T., J. S. Welch, M. Ricote, C. J. Binder, T. M. Willson, C. Kelly, J. L. Witztum, C. D. Funk, D. Conrad, and C. K. Glass.** 1999. Interleukin-4-dependent production of PPAR-gamma ligands in macrophages by 12/15-lipoxygenase. Nature **400:**378–382.

24. **Itoh, T., L. Fairall, K. Amin, Y. Inaba, A. Szanto, B. L. Balint, L. Nagy, K. Yamamoto, and J. W. Schwabe.** 2008. Structural basis for the activation of PPARgamma by oxidized fatty acids. Nat. Struct. Mol. Biol. **15:**924–931.

25. **Jobard, F., C. Lefevre, A. Karaduman, C. Blanchet-Bardon, S. Emre, J. Weissenbach, M. Ozguc, M. Lathrop, J. F. Prud'homme, and J. Fischer.** 2002. Lipoxygenase-3 (ALOXE3) and 12(R)-lipoxygenase (ALOX12B) are

26. **Kim, J. B., H. M. Wright, M. Wright, and B. M. Spiegelman.** 1998. ADD1/SREBP1 activates PPARγ through the production of endogenous ligand. Proc. Natl. Acad. Sci. U. S. A. **95:**4333–4337.

27. **Kinzig, A., M. Heidt, G. Furstenberger, F. Marks, and P. Krieg.** 1999. cDNA cloning, genomic structure, and chromosomal localization of a novel murine epidermis-type lipoxygenase. Genomics **58:**158–164.

28. **Kliewer, S. A., J. M. Lenhard, T. M. Willson, I. Patel, D. C. Morris, and J. M. Lehmann.** 1995. A prostaglandin J2 metabolite binds peroxisome proliferator-activated receptor gamma and promotes adipocyte differentiation. Cell **83:**813–819.

29. **Kliewer, S. A., S. S. Sundseth, S. A. Jones, P. J. Brown, G. B. Wisely, C. S. Koble, P. Devchand, W. Wahli, T. M. Willson, J. M. Lenhard, and J. M. Lehmann.** 1997. Fatty acids and eicosanoids regulate gene expression through direct interactions with peroxisome proliferator-activated receptors alpha and gamma. Proc. Natl. Acad. Sci. U. S. A. **94:**4318–4323.

30. **Kliewer, S. A., H. E. Xu, M. H. Lambert, and T. M. Willson.** 2001. Peroxisome proliferator-activated receptors: from genes to physiology. Recent Prog. Horm. Res. **56:**239–263.

31. **Koppen, A., R. Houtman, D. Pijnenburg, E. H. Jeninga, R. Ruijtenbeek, and E. Kalkhoven.** 2009. Nuclear receptor-coregulator interaction profiling identifies TRIP3 as a novel peroxisome proliferator-activated receptor gamma cofactor. Mol. Cell. Proteomics **8:**2212–2226.

32. **Lee, H., Y. J. Lee, H. Choi, E. H. Ko, and J. W. Kim.** 2009. Reactive oxygen species facilitate adipocyte differentiation by accelerating mitotic clonal expansion. J. Biol. Chem. **284:**10601–10609.

33. **Lehmann, J. M., L. B. Moore, T. A. Smith-Oliver, W. O. Wilkison, T. M. Willson, and S. A. Kliewer.** 1995. An antidiabetic thiazolidinedione is a high affinity ligand for peroxisome proliferator-activated receptor gamma (PPAR gamma). J. Biol. Chem. **270:**12953–12956.

34. **Lu, M., and J. Y. J. Shyy.** 2006. Sterol regulatory element-binding protein 1 is negatively modulated by PKA phosphorylation. Am. J. Physiol. Cell Physiol. **290:**C1477–C1486.

35. **Madsen, L., R. K. Petersen, M. B. Sorensen, C. Jorgensen, P. Hallenborg, L. Pridal, J. Fleckner, E. Z. Amri, P. Krieg, G. Fürstenberger, R. K. Berge, and K. Kristiansen.** 2003. Adipocyte differentiation of 3T3-L1 preadipocytes is dependent on lipoxygenase activity during the initial stages of the differentiation process. Biochem. J. **375:**539–549.

36. **Matsusue, K., J. M. Peters, and F. J. Gonzalez.** 2004. PPARβ/δ potentiates PPARγ-stimulated adipocyte differentiation. FASEB J. **18:**1477–1479.

37. **Misra, P., R. Chakrabarti, R. K. Vikramadithyan, G. Bolusu, S. Juluri, J. Hiriyan, C. Gershome, A. Rajjak, P. Kashireddy, S. Yu, S. Surapureddi, C. Qi, Y. J. Zhu, M. S. Rao, J. K. Reddy, and R. Ramanujam.** 2003. PAT5A: a partial agonist of peroxisome proliferator-activated receptor gamma is a potent antidiabetic thiazolidinedione yet weakly adipogenic. J. Pharmacol. Exp. Ther. **306:**763–771.

38. **Nagy, L., P. Tontonoz, J. G. Alvarez, H. Chen, and R. M. Evans.** 1998. Oxidized LDL regulates macrophage gene expression through ligand activation of PPARγ. Cell **93:**229–240.

39. **Ng, S. P., K. Y. Wong, L. Zhang, Z. Zuo, and G. Lin.** 2004. Evaluation of the first-pass glucuronidation of selected flavones in gut by Caco-2 monolayer model. J. Pharm. Pharm. Sci. **8:**1–9.

40. **Niedowicz, D. M., and D. L. Daleke.** 2005. The role of oxidative stress in diabetic complications. Cell Biochem. Biophys. **43:**289–330.

41. **Oberfield, J. L., J. L. Collins, C. P. Holmes, D. M. Goreham, J. P. Cooper, J. E. Cobb, J. M. Lenhard, E. A. Hull-Ryde, C. P. Mohr, S. G. Blanchard, D. J. Parks, L. B. Moore, J. M. Lehmann, K. Plunket, A. B. Miller, M. V. Milburn, S. A. Kliewer, and T. M. Willson.** 1999. A peroxisome proliferator-activated receptor gamma ligand inhibits adipocyte differentiation. Proc. Natl. Acad. Sci. U. S. A. **96:**6102–6106.

42. **Pace-Asciak, C. R., D. Reynaud, P. Demin, and S. Nigam.** 1999. The hepoxilins. A review. Adv. Exp. Med. Biol. **447:**123–132.

43. **Powell, W. S.** 2003. 15-Deoxy-$\Delta^{12,14}$-PGJ2: endogenous PPARγ ligand or minor eicosanoid degradation product? J. Clin. Invest. **112:**828–830.

44. **Rosen, E. D., and O. A. MacDougald.** 2006. Adipocyte differentiation from the inside out. Nat. Rev. Mol. Cell. Biol. **7:**885–896.

45. **Rosen, E. D., P. Sarraf, A. E. Troy, G. Bradwin, K. Moore, D. S. Milstone, B. M. Spiegelman, and R. M. Mortensen.** 1999. PPAR gamma is required for the differentiation of adipose tissue in vivo and in vitro. Mol. Cell **4:**611–617.

46. **Rosen, E. D., and B. M. Spiegelman.** 2000. Molecular regulation of adipogenesis. Annu. Rev. Cell Dev. Biol. **16:**145–171.

47. **Rosenbaum, S. E., and A. S. Greenberg.** 1998. The short- and long-term effects of tumor necrosis factor-alpha and BRL 49653 on peroxisome proliferator-activated receptor (PPAR)γ2 gene expression and other adipocyte genes. Mol. Endocrinol. **12:**1150–1160.

48. **Sarraf, P., E. Mueller, W. M. Smith, H. M. Wright, J. B. Kum, L. A. Aaltonen, A. de la Chapelle, B. M. Spiegelman, and C. Eng.** 1999. Loss-of-function mutations in PPAR gamma associated with human colon cancer. Mol. Cell **3:**799–804.

49. **Schneider, C., D. A. Pratt, N. A. Porter, and A. R. Brash.** 2007. Control of

mutated in non-bullous congenital ichthyosiform erythroderma (NCIE) linked to chromosome 17p13.1. Hum. Mol. Genet. **11:**107–113.

oxygenation in lipoxygenase and cyclooxygenase catalysis. Chem. Biol. **14:** 473–488.

50. **Schopfer, F. J., Y. Lin, P. R. Baker, T. Cui, M. Garcia-Barrio, J. Zhang, K. Chen, Y. E. Chen, and B. A. Freeman.** 2005. Nitrolinoleic acid: an endogenous peroxisome proliferator-activated receptor gamma ligand. Proc. Natl. Acad. Sci. U. S. A. **102:**2340–2345.

51. **Schulman, I. G., G. Shao, and R. A. Heyman.** 1998. Transactivation by retinoid X receptor-peroxisome proliferator-activated receptor gamma (PPARγ) heterodimers: intermolecular synergy requires only the PPARγ hormone-dependent activation function. Mol. Cell. Biol. **18:**3483–3494.

52. **Siebert, M., P. Krieg, W. D. Lehmann, F. Marks, and G. Furstenberger.** 2001. Enzymic characterization of epidermis-derived 12-lipoxygenase isoenzymes. Biochem. J. **355:**97–104.

53. **Tontonoz, P., L. Nagy, J. G. Alvarez, V. A. Thomazy, and R. M. Evans.** 1998. PPARγ promotes monocyte/macrophage differentiation and uptake of oxidized LDL. Cell **93:**241–252.

54. **Tzameli, I., H. Fang, M. Ollero, H. Shi, J. K. Hamm, P. Kievit, A. N. Hollenberg, and J. S. Flier.** 2004. Regulated production of a peroxisome proliferator-activated receptor-gamma ligand during an early phase of adipocyte differentiation in 3T3-L1 adipocytes. J. Biol. Chem. **279:**36093–36102.

55. **Walkey, C. J., and B. M. Spiegelman.** 2008. A functional peroxisome proliferator-activated receptor-gamma ligand-binding domain is not required for adipogenesis. J. Biol. Chem. **283:**24290–24294.

56. **Wolber, G., and T. Langer.** 2005. LigandScout: 3-D pharmacophores derived from protein-bound ligands and their use as virtual screening filters. J. Chem. Inf. Model. **45:**160–169.

57. **Xu, H. E., M. H. Lambert, V. G. Montana, D. J. Parks, S. G. Blanchard, P. J. Brown, D. D. Sternbach, J. M. Lehmann, G. B. Wisely, T. M. Willson, S. A. Kliewer, and M. V. Milburn.** 1999. Molecular recognition of fatty acids by peroxisome proliferator-activated receptors. Mol. Cell **3:**397–403.

58. **Yellaturu, C. R., X. Deng, L. M. Cagen, H. G. Wilcox, E. A. Park, R. Raghow, and M. B. Elam.** 2005. Posttranslational processing of SREBP-1 in rat hepatocytes is regulated by insulin and cAMP. Biochem. Biophys. Res. Commun. **332:**174–180.

59. **Yin, H., and N. A. Porter.** 2005. New insights regarding the autoxidation of polyunsaturated fatty acids. Antioxid. Redox. Signal **7:**170–184.

60. **Yoshimoto, T., and Y. Takahashi.** 2002. Arachidonate 12-lipoxygenases. Prostaglandins Other Lipid Mediat. **68–69:**245–262.

61. **Yu, K., W. Bayona, C. B. Kallen, H. P. Harding, C. P. Ravera, G. McMahon, M. Brown, and M. A. Lazar.** 1995. Differential activation of peroxisome proliferator-activated receptors by eicosanoids. J. Biol. Chem. **270:**23975–23983.

62. **Yu, Z., C. Schneider, W. E. Boeglin, and A. R. Brash.** 2005. Mutations associated with a congenital form of ichthyosis (NCIE) inactivate the epidermal lipoxygenases 12R-LOX and eLOX3. Biochim. Biophys. Acta 1686 **3:**238–247.

63. **Yu, Z., C. Schneider, W. E. Boeglin, and A. R. Brash.** 2006. Human and mouse eLOX3 have distinct substrate specificities: implications for their linkage with lipoxygenases in skin. Arch. Biochem. Biophys. **455:**188–196.

64. **Yu, Z., C. Schneider, W. E. Boeglin, and A. R. Brash.** 2007. Epidermal lipoxygenase products of the hepoxilin pathway selectively activate the nuclear receptor PPARα. Lipids **42:**491–497.

65. **Yu, Z., C. Schneider, W. E. Boeglin, L. J. Marnett, and A. R. Brash.** 2003. The lipoxygenase gene ALOXE3 implicated in skin differentiation encodes a hydroperoxide isomerase. Proc. Natl. Acad. Sci. U. S. A. **100:**9162–9167.

66. **Zhang, Y., L. Yin, and F. B. Hillgartner.** 2003. SREBP-1 integrates the actions of thyroid hormone, insulin, cAMP, and medium-chain fatty acids on ACCα transcription in hepatocytes. J. Lipid Res. **44:**356–368.

67. **Zhu, M., S. Rajamani, J. Kaylor, S. Han, F. Zhou, and A. L. Fink.** 2004. The flavonoid baicalein inhibits fibrillation of α-synuclein and disaggregates existing fibrils. J. Biol. Chem. **279:**26846–26857.